J. KSIAM **Vol.11**, No.1, 71-83, 2007

EFFECT OF PARTITION AND SPECIES DIFFUSIVITY ON DOUBLE DIFFUSIVE CONVECTION OF WATER NEAR DENSITY MAXIMUM

S SIVASANKARAN AND P KANDASWAMY

ABSTRACT. The double diffusive convection of cold water in the vicinity of its density maximum in a rectangular partitioned enclosure of aspect ratio 5 with isothermal side walls and insulated top and bottom is studied numerically. A thin partition is attached to the hot wall. The species diffusivity of the fluid is assumed to vary linearly with concentration. The governing equations are solved by finite difference scheme. The effects of position and height of the partition, variable species diffusivity and enclosure width are analyzed for various hot wall temperatures. It has been found that adding partition on the hot wall reduces the heat transfer. The density inversion of the water has a great influence on the natural convection. When increasing species diffusivity parameter heat and mass transfer rate is decreased.

2000 Mathematics Subject Classification. 76R10, 76M20, 80A20.

Keywords. Convection, Density Maximum, Partition enclosure, Species diffusivity

1. INTRODUCTION

Double diffusive convection in complex geometry has attracted the interest of several researchers. Double diffusive convection occurs in a very wide range of fields such as Oceanography, Astrophysics, Geology, Biology, Chemical process etc. Most works about cavities of complex geometry deal with partitions fitted to insulated walls. Cavities with baffles on their active walls have been less studied. Heat transfer in partially divided enclosures has received attention primarily due to its many engineering and physical applications such as in the design of energy efficient building, reduction of heat loss from flat plate solar collectors, natural gas storage tank, crystal manufacturing and metal solidification processes. This study describes the effect of a thin baffle at the hot wall of a water filled, differentially heated rectangular enclosure. Braga and Viskanta [1992] made an experimental and theoretical investigation of transient natural convection heat transfer of water near its maximum density in a rectangular cavity. They found two counter rotating eddies in all experiments caused by density inversion. Dagtekin and Oztop [2001] analyzed numerically the effect of positions and height of two partitions on natural convection within an enclosure. They found that the effect of the position of the partitions on the fluid flow more than that on heat transfer.

Frederick [1989] investigated numerically the natural convection of differentially heated cavity with a diathermal partition on its cold wall. He also described the results for inclined and rectangular cavity. He concluded that the partition causes convection suppression and heat transfer reductions upto 47% relative to the undevided cavity at the same Rayleigh number. Hyun and Lee [1990] investigated double

diffusive convection in a rectangular cavity with imposed temperature and concentration gradients in the horizontal direction. They found mean Sherwood number decreases monotonically as buoyancy ratio increases. Lin and Nansteel [1987] analyzed numerically the steady natural convection of cold water near the density extremum in a vertical annulus. They found that density inversion phenomena are altered substantially by curvature of the annulus. Mamou et al. [1996] studied both analytically and numerically double diffusive natural convection in a rectangular slot subject to uniform heat and mass fluxes along the vertical sides. They found a good agreement between the analytical predictions and the numerical simulation.

Robillard and Vasseur [1981] studied maximum density effect of water on laminar natural convection in a rectangular cavity with a convective boundary. Tasnim and Collins [2004] numerically investigated the effect of attaching a high conducting thin baffle on the hot wall of a square cavity. They concluded that adding baffle on the hot wall increase the rate of heat transfer about 31.46% compared with a wall without baffle. Vasseur and Robillard [1980] investigated the inversion of flow patterns caused by the maximum density of water at 4^0C enclosed in rectangular cavities. Wang et al. [1999] studied numerically the natural convection in a partially divided rectangular enclosure and conclude that the location of the divider effect the heat transfer performance and height of the divider influences the heat transfer significantly. Zimmerman and Acharya [1987] numerically studied natural convection in an enclosure with finitely conducting baffles. They found out growing and spreading of the counter clockwise vortex in the entire rectangular cavity appears to be a slower process than in the case of square cavity.

There is a considerable number of numerical studies concerning on the double diffusive convection in two dimensional partitioned enclosures. However such studies are typically devoted to a linear density temperature dependent fluid. For a number of fluids, the density-temperature relation exhibits an extremum. Because the coefficient of thermal expansion changes sign at this extremum, simple linear relations for density as a function of temperature are inadequate near the extremum. The most common fluid, water has such behaviour. Sundaravadivelu and Kandaswamy [2000] analyzed the natural convection flow of pure water around its temperature of maximum density existing between temperatures 273 K and 285 K by using a non-linear temperature dependent equation for density in a square cavity. In the present study we continue to examine the effect of position and length of the baffle and species diffusivity in rectangular partitioned enclosure with different hot wall temperatures using a non linear density temperature profile.

2. MATHEMATICAL FORMULATION

The physical system under consideration is a two dimensional rectangular partitioned enclosure of width W and height H filled with water and some mass, Fig. 1. The vertical side walls of the enclosure are isothermal but maintained at different temperatures θ_h (hot wall) and θ_c (cold wall) with $\theta_h > \theta_c$. The horizontal

walls are thermally insulated. A very thin adiabatic partition of length L_B attached on the hot wall at a height H_B from the bottom of the enclosure. The concentration level of mass is taken to be c_2 at $y = 0$ and c_1 at $y = W$, where $c_2 < c_1$. The species diffusivity of the fluid D is assumed to vary linearly with concentration as $D = D_o[1 - a(c - c_o)]$, where a is the concentration coefficient of the diffusion and the subscript o refers to the reference state. A density-temperature 4^{th} degree polynomial fit of the form $\rho = \rho_o\left[1 - \sum_{i=1}^{4}(-1)^i\beta_i(\theta - \theta_c)^i - \beta_5(c - c_2)\right]$ for pure water for the data available in the literature is found to be an ideal one with $\rho_o = 9.9984 \times 10^2$, $\beta_1 = 6.8143 \times 10^{-5}$, $\beta_2 = 9.9901 \times 10^{-6}$, $\beta_3 = 2.7217 \times 10^{-7}$, $\beta_4 = 6.7252 \times 10^{-9}$, and $\beta_5 = 3 \times 10^{-3}$. A graphical representation of the relation provided in Fig. 2 gives a clear demonstration of the fit. Further there is no chemical reaction between the mass and the fluid. The cartesian coordinates (x, y) with their corresponding velocity components (u, v) are as indicated in Fig. 1.

The nondimentional vorticity-stream function formulation of the laminar two-dimensional incompressible flow of the fluid under consideration are

$$\frac{\partial T}{\partial \tau} + U\frac{\partial T}{\partial X} + V\frac{\partial T}{\partial X} = \frac{1}{P_r}\nabla^2 T \tag{1}$$

$$\frac{\partial C}{\partial \tau} + U\frac{\partial C}{\partial X} + V\frac{\partial C}{\partial X} = \frac{1}{Sc}\left\{[1 - \lambda C]\nabla^2 C - \lambda\left[\left(\frac{\partial C}{\partial X}\right)^2 + \left(\frac{\partial C}{\partial Y}\right)^2\right]\right\} \tag{2}$$

$$\frac{\partial \zeta}{\partial \tau} + U\frac{\partial \zeta}{\partial X} + V\frac{\partial \zeta}{\partial Y} = \sum_{i=1}^{4} i(-1)^i Gr_i^T \frac{\partial T}{\partial Y} + Gr_5^C \frac{\partial C}{\partial Y} + \nabla^2 \zeta \tag{3}$$

$$\nabla^2 \Psi = -\zeta \tag{4}$$

where $U = -\dfrac{\partial \Psi}{\partial Y}$, $V = \dfrac{\partial \Psi}{\partial X}$ and $\zeta = \dfrac{\partial U}{\partial Y} - \dfrac{\partial V}{\partial X}$

with the initial and boundary conditions

$\tau = 0$; $\zeta = \psi = 0$; $T = C = 0$; $0 \le X \le Ar$; $0 \le Y \le 1$

$\tau > 0$; $\Psi = \dfrac{\partial \Psi}{\partial X} = 0$; $\dfrac{\partial T}{\partial X} = \dfrac{\partial C}{\partial X} = 0$; $X = 0$, Ar & on the baffle; $0 \le Y \le 1$

$\Psi = \dfrac{\partial \Psi}{\partial X} = 0$; $T = 1$, $C = 0$; $Y = 0$; $0 \le X \le Ar$

$\Psi = \dfrac{\partial \Psi}{\partial X} = 0$; $T = 0$, $C = 1$; $Y = 1$; $0 \le X \le Ar$

The following non-dimensional variables are used to transform the dimensional equations to non-dimensional form are

$$X = \frac{x}{W}, \quad Y = \frac{y}{W}, \quad U = \frac{u}{\nu/W}, \quad V = \frac{v}{\nu/W}, \quad \tau = \frac{t}{W^2/\nu}, \quad \Psi = \frac{\psi}{\nu},$$

$$\zeta = \frac{\omega}{\nu/W^2}, \qquad T = \frac{\theta - \theta_c}{\theta_h - \theta_c} \qquad C = \frac{c - c_o}{c_1 - c_2} \text{ where } \theta_h > \theta_c \text{ and } c_1 > c_2.$$

The non-dimensional parameters that appear in the equations are the thermal Grashof numbers $Gr_i^T = (g\beta_i(\theta_h - \theta_c)^i W^3)/\nu^2$, $i = 1, 2, 3, 4$, the species Grashof number $Gr_5^C = (g\beta_5(c_1 - c_2)W^3/\nu^2$, the Prandtl number $Pr = \nu/\alpha$, the Schmidt number $Sc = \nu/D$, the aspect ratio $Ar = H/W$, and the species diffusivity parameter $\lambda = a(c_1 - c_2)$, where g is gravity, α is the thermal diffusivity, β is the coefficient of thermal expansion and ν is the kinematic viscosity. The local Nusselt number and Sherwood number are defined by $Nu = \frac{\partial T}{\partial Y}\big|_{Y=0}$ and $Sh = \frac{\partial C}{\partial Y}\big|_{Y=1}$, resulting in the average Nusselt number and Sherwood number as

$$\overline{Nu} = \frac{1}{Ar}\int_0^{Ar} Nu\, dX \quad \text{and} \quad \overline{Sh} = \frac{1}{Ar}\int_0^{Ar} Sh\, dX.$$

3. THE METHOD OF SOLUTION

Numerical solution of the governing equations is obtained using finite difference method. An approximate solution of the equations is obtained at a finite number of grid points distributed over the rectangular enclosure, having the coordinates $x = ih, y = ik$, and at discrete times $\tau = n\Delta\tau$ where i, j, n are integers and h, k are small increments. Here we find the solution for a 51×251 square mesh with $h = k$. Knowing all quantities at a time $\tau = n\Delta\tau$ (the initial condition corresponds to the special case $n = 0$), an Alternating Direction Implicit (ADI) method is employed to find the temperature and velocity values at the interior grid points in the next time level $(n + 1)\Delta\tau$. For this forward difference approximation is used for time derivatives and central difference approximation are used for all space derivatives. ADI method is a two step approach and requires minimal computer storage and is quite accurate. This approach involves the alternate use of two different finite difference approximations to the two dimensional problem in space. Solutions with more finer meshes ($61 \times 301 - 101 \times 501$) have produced in significant improvement results less than 1% in velocity and temperature fields with a five fold increase in computer time. Hence the 51×251 mesh was opted as the ideal one.

The method of Successive Over Relaxation (SOR) gives faster convergence than other relaxation methods. We fix the relaxation parameter to be 1.5. The velocity components $U = -\frac{\partial \Psi}{\partial Y}$ and $V = \frac{\partial \Psi}{\partial X}$ are then found using central difference approximations. After finding all the values at a particular level, the values at the higher levels are similarly computed. This computational cycle is repeated for each of the next levels and steady state solution is obtained when the convergent criteria $|\Phi_{i,j,n} - \Phi_{i,j,n+1}| < \epsilon (= 10^{-5})$ for temperature, vorticity, species concentration and stream function have been met.

4. RESULTS AND DISCUSSIONS

The effect of concentration dependent species diffusivity on the double diffusive convective motion of cold water at temperatures around its density maximum is investigated numerically within a rectangular partitioned enclosure. The solute taken into consideration is assumed to posses the property of raising the temperature of maximum density. By invoking a fourth-order approximation for density-temperature-concentration relation, results were obtained for various values of parameters like, partition height and length, diffusivity parameter and width of an enclosure. Though the problem is unsteady the results are discussed after the final steady state is reached. The results of the investigations for cavity dimension namely width = 8 mm are presented in the form of streamlines, isotherms, isoconcentration lines, velocity profiles and average Nusselt and Sherwood numbers for various hot wall temperatures between 279 K and 285 K. The cold wall is always maintained at temperature 273 K.

Fig. 3(a) drawn to predict the fluid motion and the resulting temperature and concentration distribution for hot wall temperature (θ_h) of 279 K and $\lambda = 0.001$. The stream lines shows a single counter clockwise rotating eddy and occupies the whole enclosure. This is found to be unusual when compared to common vertical flows where density is assumed as linearly varying with temperature. The resulting isotherms clearly show that the heat transfer mode is changed from conduction to convection. The upper region of the isotherms are pushed towards the cold wall and the lower region towards the hot wall. This results in a single buoyancy-induced cell.

When hot wall temperature is raised to 281 K, Fig. 3(b), there exists a small clockwise rotating eddy near the top corner of hot wall side. This is due to density inversion. As the hot wall temperature increases the size of the hot wall side cell is increased because the maximum density plane is moved from hot wall side to cold wall. The heat and mass transfer process are found to be disturbed due to the resulting bicellular flow structure. For $\theta_h = 283$ K the cell rotating in the clockwise direction in the above bicellular flows, is now found to grow in its size by suppressing its counterpart since the maximum density plane is very near to the cold wall. The same behaviour of flow was observed with increasing the species diffusivity parameter $\lambda = 0.5$. Hence the graphs are plotted only for the case $\lambda = 0.001$.

Figs. 4(a-c) show the streamlines, isotherms and isoconcentrationlines for different hot wall temperatures with baffle at height $H_B = 1/2$ and length $L_B = 1/2$. It is clearly seen from these figures that the baffle affected the streamlines, isotherms and isoconcentrationlines. The flow pattern is affected very much. The eddy in Fig. 4(a) circulates in counter clockwise direction and occupies the whole cavity. The movement of the eddy is downward along the hot wall and upward along the cold wall due to high density resulting from anomalous density behaviour. Difference in temperature, being the cause for such fluid motion found, is distributed across the isothermal walls of the cavity. The eddy for $\theta_h = 279$ K, occupies the whole cavity with two secondary eddies separated by baffle, that is, one above the baffle and another below the baffle. The concentration profiles are more deviated from the baffle when the density is decreasing. For $\theta_h = 281$ K, there exists a small vortex below the baffle as well as a

large clockwise rotating vortex appear above the baffle because the effect of density inversion. Still increasing the hot wall temperature $\theta_h = 283K$, two counter rotating cells exists the hot cell grows in size and suppressing its counterpart. The cold wall vortex also separate into two cells.

We observe that the hot wall side vortices grow in size with increasing temperature gradient by suppressing their respective cold wall side vortices. Therefore a transition in the heat flow behaviour from conduction to convection mode is switched on. Hence the average heat transfer rate is found to increase almost monotonically with increasing hot wall temperature above 283 K. Figs. 5(a & b) show that the streamlines pattern for different hot wall temperatures and $\lambda = 0.001$ with partition at $H_B = 1/4$ & $3/4$ and $L_B = 1/2$. When baffle is at $H_B = 3/4$, we observed that the behaviour of flow, heat and concentration structures above the baffle is like as the structure below the baffle when baffle at $H = 1/4$. Figs. 6(a & b) show the streamlines for different hot wall temperature and $\lambda = 0.001$ with partition at $H_B = 1/2$ & $L_B = 1/4$ & $3/4$. For the baffle length $L_B = 1/4$ there is no considerable effect on heat and mass transfer and there is a very small change in flow pattern is observed. Further increasing the baffle length $L_B = 3/4$, the flow pattern, isotherms and isoconcentrationlines are more affected than the other two cases like $L_B = 1/4$ & $1/2$. The flow structure is totally affected due to narrow gap and behaves like almost two separate regions.

The investigations are also carried out in a cavity with still higher dimension (20 *mm*) are reported. Figs. 7(a-c) show the streamlines, isotherms and isoconcentrationlines for different hot wall temperature, $\lambda = 0.001$ and $L = 20$ *mm* with baffle at height $H_B = 1/2$ and length $L_B = 1/2$. From all these figures we observe that in general a high buoyancy force results inside the cavity, which in turn drives the fluid motion at a higher velocity. The resulting convection process is found to be more vigorous than in the case of 8 *mm* cavity. Their respective isotherms and isoconcentrationlines are found to be distorted largely. The attraction of isotherms towards the cold wall and hence the formation of thermal boundary layer is clear in Fig. 7(a), showing that considerable amount of heat is propagated form hot wall to cold wall across an enclosure. As the cavity dimension is increased, circulation rate of the eddy becomes larger and the flow vigorous is increased significantly. We also found average Nusselt number is increased.

In order to evaluate how the presence of the partition affects the average Nusselt number along the hot wall, average Nusselt number is plotted as a function of partition length and height for different hot wall temperatures, see Figs. (8-10). Figs. 8(a-c) show the average Nusselt number for $\lambda = 0.001$ and different partition heights and lengths. We see that average Nusselt number decreases with increasing baffle length before density maximum and after the density maximum average Nusselt number is increased. Figs. 9(a-c) show the average Sherwood number for different baffle positions and $\lambda = 0.001$. When changing the position of the partition the effect on average Sherwood number is very small. As increasing the partition length we got some remarkable effects on average Sherwood number. Comparing these three figures, the range of variation of average Sherwood number is small for all values of λ.

Average Nusselt and Sherwood numbers for different λ values are depicted in the Figs. 10(a & b). As λ is increased average Nusselt and Sherwood numbers decrease. There is no considerable variation in heat transfer rate after density inversion. Fig. 11 shows the time history of the average Nusselt number and Sherwood number for various hot wall temperatures. As time evolves the particles near the hot wall have higher temperature and so the heat transfer rate starts decreasing thus we get a sudden fall in the values of $\overline{Nu}$ as seen in the graph. Finally the steady state is reached and the $\overline{Nu}$ is seen to be constant. Average Nusselt number is decreased when increasing the hot wall temperature after one certain stage i.e., at the density maximum average Nusselt number is increased. The mid height velocity profiles are depicted in the Fig. 12 for different hot wall temperatures without partition, reveal the existence of multicellular counter acting flow behaviour from their respective bidirectional velocity distributions.

5. CONCLUSIONS

From the results it is concluded that the multiple fluid vortices exist inside the enclosure due to temperature of maximum density and the size of these vortices strongly depend on the hot wall temperature. The average heat transfer rate calculated is found to be an increasing function of hot wall temperatures. The partition reduces the heat transfer. The positions of the partition have more effects on fluid flow than heat transfer. It is clearly demonstrated that the density inversion of water has a great influence on the natural convection and heat and mass transfer rate is reduced around the density maximum region. The flow structure is totally different from the classical natural convection model which employ the linear density temperature relation. Heat and mass transfer rate is decreased when species diffusivity parameter is increased.

References

[1] S.L.Braga and R.Vistanta, Transient natural convection of water near its density extremum in a rectangular cavity, Int. J. Heat Mass Transfer, 35 (1992), 861-875.

[2] I.Dagtekin and H.F.Oztop, Natural Convection Heat Transfer by Heated Partitions within Enclosure, Int. Comm. Heat Mass Transfer, 28 (2001), 823-834.

[3] R.L.Frederick, Natural Convection in an inclined square enclosure with a partition attached to its cold walls, Int. J. Heat Mass Transfer, 32 (1989), 87-94.

[4] J.M.Hyun and J.W.Lee, Double-diffusive convection in a rectangle with cooperating horizontal gradients of temperature and concentration, Int. J. Heat Mass Transfer, 33 (1990), 1605-1617.

[5] D.S.Lin and M. W.Nansteel, Natural Convection in a Vertiacal Annulus Containing Water near the Density Maximum, J. Heat Transfer, 109 (1987), 899-905.

[6] M.Mamou, P.Vasseur and E.Bilgen, Analytical and numerical study of double-diffusive convection in a vertical enclosure, Heat and Mass Transfer, 32 (1996), 115-125.

[7] L.Robillard and P.Vasseur, Transient Natural Convection Heat Transfer of Water with Maximum Density Effect and Supercooling, J. Heat Transfer, 103 (1981), 528-534.

[8] K.Sundaravadivelu and P.Kandaswamy, Double Diffusive Non-linear convection in Square cavity , J. Fluid Dynamics Research, 27 (2000), 291-303.

[9] S.H.Tasnim and M.R.Collins, Numerical Analysis of Heat Transfer in a Square Cavity with a Baffle on the Hot Wall, Int. Comm. Heat Mass Transfer, 31 (2004), 639-650.

[10] P.Vasseur and L.Robillard, Transient Natural Convection Heat Transfer in a Mass of Water Cooled Through 4^0C, Int. J. Heat Mass Transfer, 23 (1980), 1195-1205.

[11] S.-G.Wang, T.-Y.Li and P.-T.Hsu, Natural Convection of Micro-polar fluid in a Partially Divided Enclosure, Acta Mechanica, 136 (1999), 41-53.

[12] E.Zimmerman and S.Acharya, Free Convection heat transfer in a partially divided vertical enclosure with conducting end walls, Int. J. Heat Mass Transfer, 30 (1987), 319-331.

UGC-DRS Center for Fluid Dynamics, Department of Mathematics,
Bharathiar University, Coimbatore-641046, Tamil Nadu, India
E-mail address: pgkswamy@yahoo.co.in

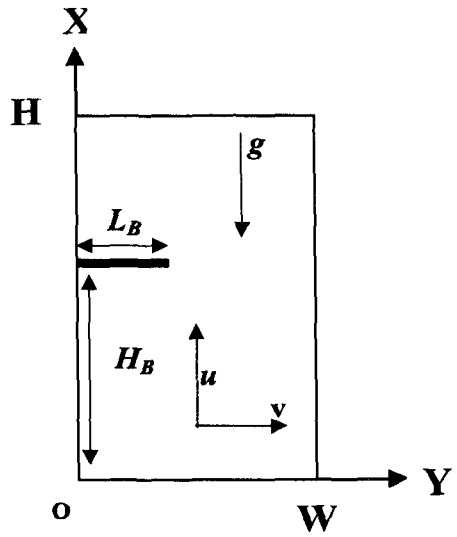

Fig. 1 Physical Configuration

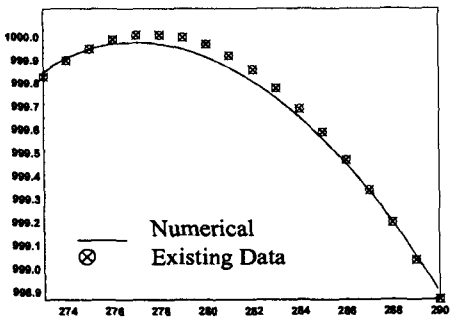

Fig.2 Temperature dependence of density

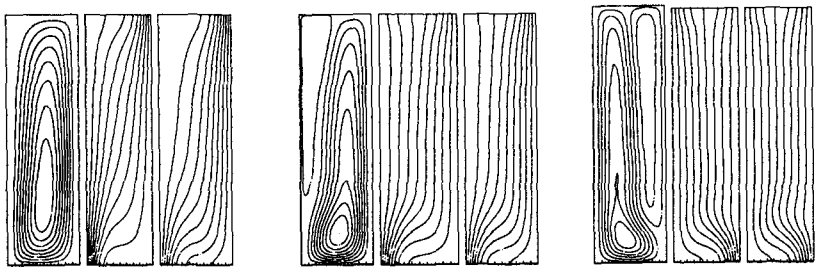

(a) θ_h= 279 K (b) θ_h= 281 K (c) θ_h= 283 K

Fig. 3 Streamlines, isotherms and isoconcentrationlines for λ=0.001 and without baffle

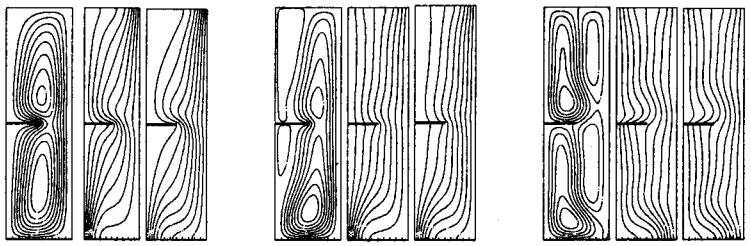

(a) θ_h= 279 K (b) θ_h= 281 K (c) θ_h= 283 K

Fig. 4 Streamlines, isotherms and isoconcentrationlines for λ=0.001 and baffle at H_B=L_B=1/2

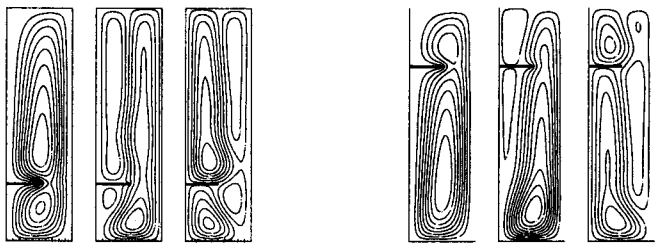

279 K 281 K 283 K 279 K 281 K 283 K

(a) H_B=1/4 (b) H_B=3/4

Fig. 5 Streamlines for λ=0.001 and baffle at L_B=1/2

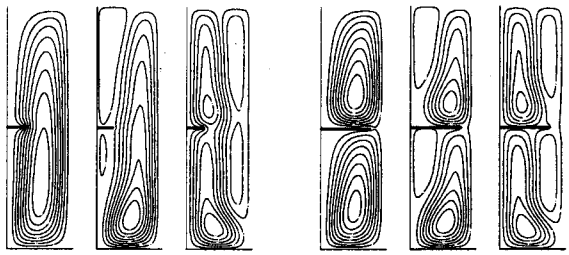

279 K 281K 283 K 279 K 281K 283 K

(a) L_B=1/4 (b) L_B=3/4

Fig. 6 Streamlines for λ=0.001 and baffle at H_B=1/2

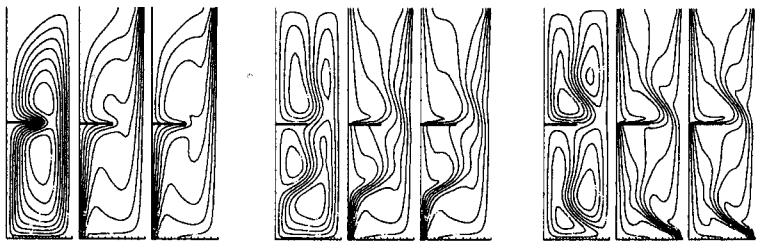

(a) θ_h= 279 K (b) θ_h= 281 K (c) θ_h= 283 K

Fig. 7 Streamlines, isotherms and isoconcentrationlines for λ=0.001, L=20mm & baffle at H_B= L_B=1/2

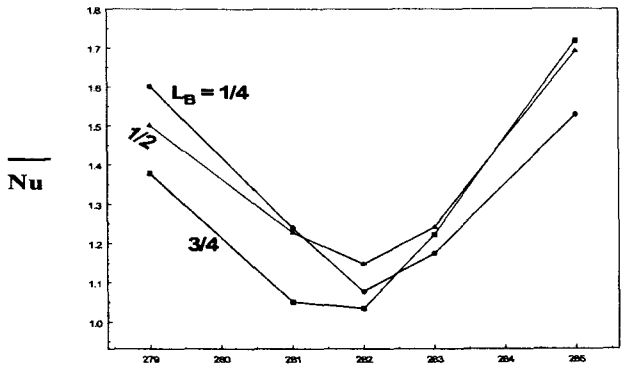

(a) H_B=1/4

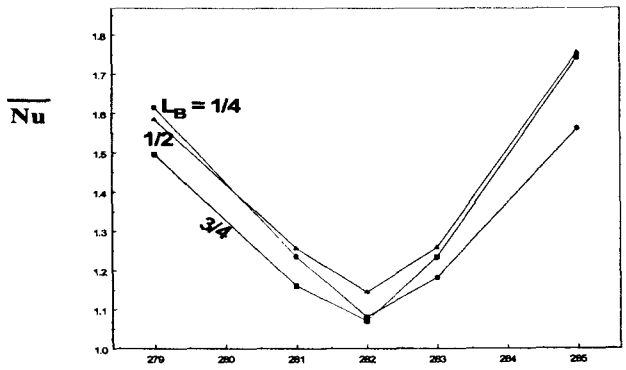

(b) H_B=1/2

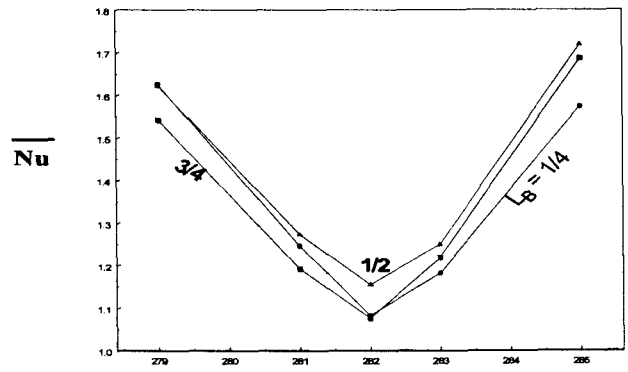

(c) H_B=3/4

Fig. 8 Average Nusselt number for λ = 0.001

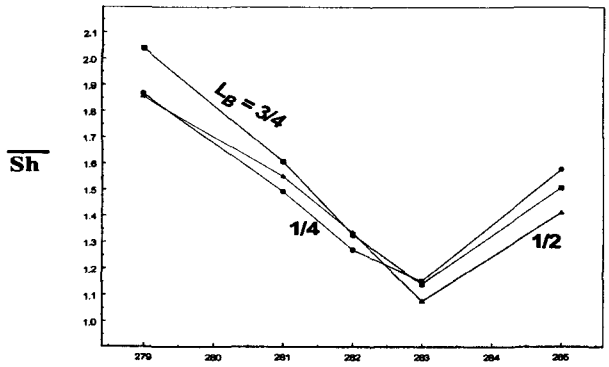

(a) H_B=1/4

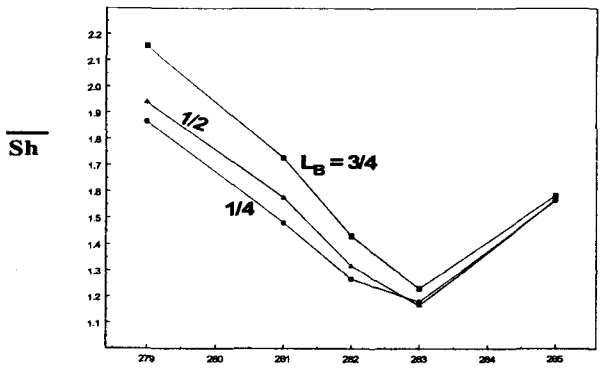

(b) H_B=1/2

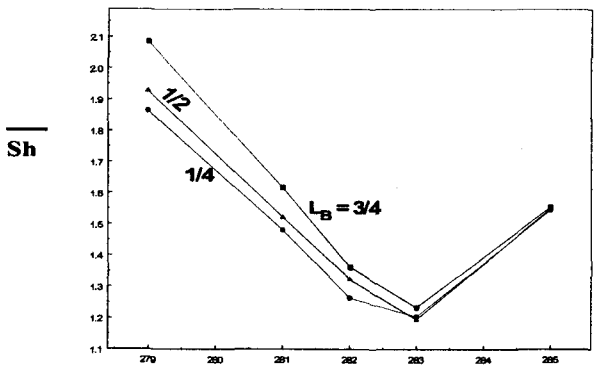

(c) H_B=3/4

Fig. 9 Average Sherwood number for $\lambda = 0.001$

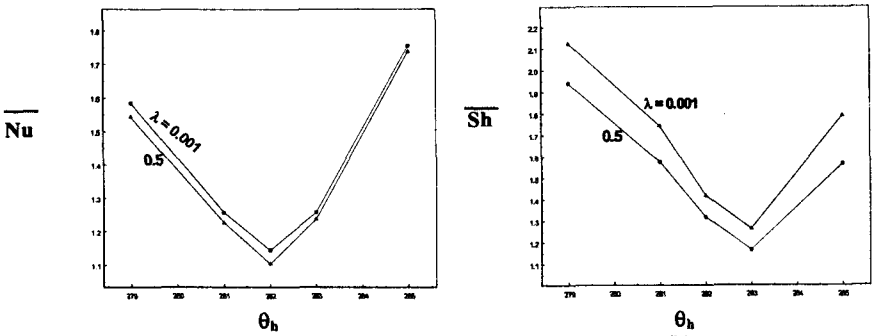

Fig. 10 Average Nusselt and Sherwood number for different λ & baffle at $H_B = L_B = ½$.

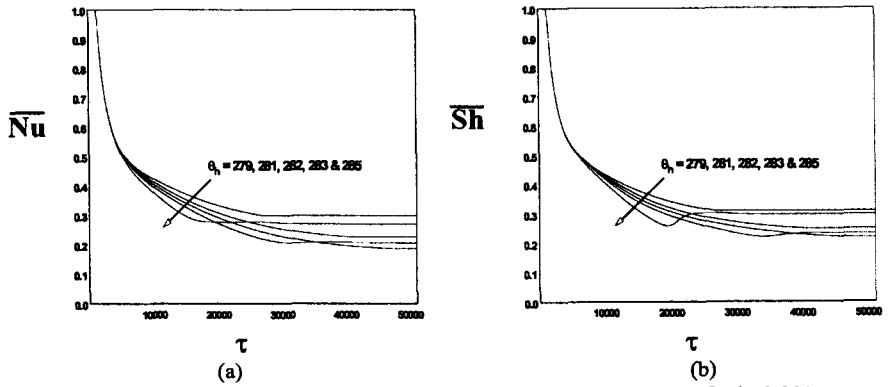

Fig. 11 Time history of average Nusselt and Sherwood numbers for λ=0.001 and baffle at $H_B=L_B$ = 1/2.

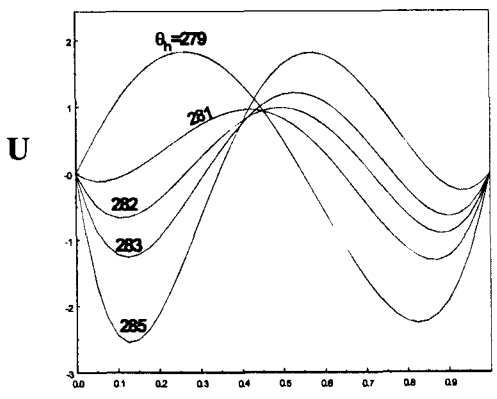

Fig. 12 Mid-height velocity profiles for λ=0.001